

Hierarchical Regularizers for Mixed-Frequency Vector Autoregressions

Alain Hecq Marie Ternes* Ines Wilms†

Department of Quantitative Economics, Maastricht University

December 23, 2024

Abstract

Mixed-frequency Vector AutoRegressions (MF-VAR) model the dynamics between variables recorded at different frequencies. However, as the number of series and high-frequency observations per low-frequency period grow, MF-VARs suffer from the “curse of dimensionality”. We curb this curse through a regularizer that permits various hierarchical sparsity patterns by prioritizing the inclusion of coefficients according to the recency of the information they contain. Additionally, we investigate the presence of nowcasting relations by sparsely estimating the MF-VAR error covariance matrix. We study predictive Granger causality relations in a MF-VAR for the U.S. economy and construct a coincident indicator of GDP growth.

Keywords: mixed-frequencies, vector autoregressions, high-dimensionality, group lasso, variable selection, coincident indicators

JEL codes: C55, C32

*Corresponding author: Marie Ternes, Maastricht University, School of Business and Economics, P.O. Box 6200 MD Maastricht, The Netherlands, Email: m.ternes@maastrichtuniversity.nl

†IW gratefully acknowledges funding from the European Union’s Horizon 2020 research and innovation programme under the Marie Skłodowska-Curie grant agreement No 832671.

1 Introduction

Vector AutoRegressive (VAR) models are a cornerstone for modeling multivariate time series; for studying dynamics between multiple series and for forecasting. However, standard VARs require all component series to enter the model at the same frequency, while in practice macro and financial series are typically recorded at different frequencies; quarterly, monthly, weekly or daily for instance. One could aggregate the high-frequency variables to one common low frequency and continue the analysis with a standard VAR, but such a practice wastes valuable information for policy makers contained in the high-frequency data that closely track the state of the economy in real time. Mixed-frequency (MF) models, instead, exploit the information available in series recorded at different frequencies. One commonly used MF models is the MIXed DATA Sampling (MIDAS) regression (Ghysels et al., 2004). While the literature first focused on a single-equation framework for modelling the low-frequency variable, the multivariate extension by Ghysels (2016) enabled one to model the relations between high- and low-frequency series in a mixed-frequency VAR (MF-VAR) system.¹

A serious complication with MF-VARs is that they are severely affected by the “curse of dimensionality”. This curse arises due to two different sources. First, the number of parameters grows quadratically with the number of component series, just like for standard VARs. Secondly, specific to the MF-VAR, we have many high-frequency observations per low-frequency observation, which each enter as different component series in the model, thereby adding to the dimensionality. Without further adjustments, one would be limited to MF-VARs with few time series and/or with a small number of high-frequency observations per low-frequency observation.

This curse of dimensionality has mostly been addressed through mixed-frequency factor models (e.g., Marcellino and Schumacher, 2010; Foroni and Marcellino, 2014; Andreou et al., 2019) or Bayesian estimation (e.g., Schorfheide and Song, 2015; McCracken et al., 2015; Ghysels, 2016; Götz et al., 2016). Sparsity-inducing convex regularizers form an appealing alternative (see Hastie et al., 2015 for an introduction), but despite their popularity in regression and standard VAR settings (e.g., Hsu et al., 2008; Basu et al., 2015; Callot et al., 2017; Derimer et al., 2018; Smeekees and Wijler, 2018; Barigozzi and Brownlees, 2019; Hecq et al., 2019), they have only been rarely explored as a tool for dimension reduction in mixed-frequency models. An exception is Babii et al. (2020) who recently used the sparse-group lasso to accommodate the dynamic nature of high-dimensional, mixed-frequency data. Nonetheless, they address univariate MIDAS regressions, leaving convex regularization of MF-VARs unexplored.

¹Alternatively to the MF-VAR system of Ghysels (2016), MF-VARs can be accommodated within the framework of state-space models (e.g., Kuzin et al., 2011; Foroni and Marcellino, 2014; Schorfheide and Song, 2015; Brave et al., 2019; Gefang et al., 2020; Koelbl and Deistler, 2020). In this paper, we contribute to the literature stream of Ghysels (2016) as the MF-VAR system allows for the application of standard VAR tools such as Granger causality to the mixed-frequency setting which will be discussed in Section 2.

Our paper’s first contribution concerns the introduction of a novel convex regularizer for MF-VAR systems by which we fill this gap. To this end, we propose a mixed-frequency extension of the lasso (Tibshirani, 1996) that accounts for covariates at different (high-frequency) lags being temporally ordered. We build upon the group lasso with nested groups (Nicholson et al., 2020), and encourage various flexible hierarchical sparsity patterns that prioritize the inclusion of coefficients according to – amongst others – the recency of the information the corresponding series contains about the state of the economy. Our modelling framework is general enough to incorporate other priority structures, for instance based on seasonality, practitioners may want to impose.

In addition to the development of a new MF-VAR with hierarchical lag structure, our paper investigates the presence of nowcasting restrictions in a high-dimensional mixed-frequency setting. According to Eurostat’s glossary, a nowcast is “*a rapid [estimate] produced during the current reference period [, say T^* a particular quarter,] for a hard economic variable of interest observed for the same reference period [T^*]*” (Eurostat: Statistics Explained, 2014). In this narrow sense, and contrarily to forecasting, nowcasting makes use of all available information becoming available between (and strictly speaking not including) $T^* - 1$ and T^* . Mixed-frequency models are consequently obvious and necessary tools for such investigations. Götz and Hecq (2014) show that nowcasting in (low-dimensional) MF-VARs can be studied through contemporaneous Granger causality tests; by testing the null of a block diagonal error covariance matrix of the MF-VAR. We build on Götz and Hecq (2014) to study nowcasting relations in high-dimensional MF-VARs by sparsely estimating the covariance matrix of the MF-VAR errors. Its sparsity pattern then provides evidence on those high-frequency variables (i.e. the series and their particular time period) one can use to build coincident indicators for the low-frequency main economic indicators.

In a simulation study, we find that the hierarchical regularizer performs well in terms of estimation accuracy and variable selection when compared to alternative methods. Furthermore, we accurately retrieve nowcasting relations between the low- and high-frequency variables by sparsely estimating the error covariance matrix. In the application, we study a high-dimensional MF-VAR for the U.S. economy using quarterly, monthly and weekly indicators. We apply the hierarchical regularizer to characterize the predictive Granger causality relations through a network analysis. Moreover, we investigate which high-frequency economic series nowcast quarterly U.S. real gross domestic product (GDP) growth and use those to construct a reliable coincident indicator of GDP growth.

The remainder of this paper is structured as follows. Section 2 introduces the MF-VAR with hierarchically structured parameters and defines the nowcasting causality relations, Section 3 describes the regularized estimation procedure for MF-VARs and nowcasting causality. Section 4 shows the results on the simulation study, Section 5 on the empirical application of the U.S. economy. Section 6 concludes.

2 Mixed-Frequency VARs

We start from Ghysels' (2016) mixed-frequency VAR systems and include d different high-frequency components. Let $\mathbf{y}(t)$ denote a k_L -dimensional vector collecting the low-frequency variables for $t = 1, \dots, T$. Further, let $\mathbf{x}^{m_1}(t), \mathbf{x}^{m_2}(t), \dots, \mathbf{x}^{m_d}(t)$ denote the d different, multivariate high-frequency components with m_1, m_2, \dots, m_d number of high-frequency observations per low-frequency period t , respectively. Without loss of generality, we take $m_1 < m_2 < \dots < m_d$. For instance, in a quarter/month/weekly-example $m_1 = 3$ and $m_2 = 12$. Let each component contain k_1, k_2, \dots, k_d time series of the same high-frequency, respectively. To be precise, each high-frequency component is given by

$$\mathbf{x}^{m_i}(t) = [x_1(t, m_i), \dots, x_1(t, 1), \dots, x_{k_i}(t, m_i), \dots, x_{k_i}(t, 1)]' \in \mathbb{R}^{m_i \cdot k_i} \quad \text{for } i = 1, \dots, d,$$

where the couple (t, j) indicates higher-frequency period $j = 1, \dots, m_i$ during the low-frequency period t .²

The MF-VAR $_K(\ell)$ for a lag length of $\ell = 1$ is then given by

$$\begin{pmatrix} \mathbf{y}(t) \\ \mathbf{x}^{m_1}(t) \\ \mathbf{x}^{m_2}(t) \\ \vdots \\ \mathbf{x}^{m_d}(t) \end{pmatrix} = \mathbf{B} \times \begin{pmatrix} \mathbf{y}(t-1) \\ \mathbf{x}^{m_1}(t-1) \\ \mathbf{x}^{m_2}(t-1) \\ \vdots \\ \mathbf{x}^{m_d}(t-1) \end{pmatrix} + \begin{pmatrix} \mathbf{u}(t) \\ \mathbf{u}^{m_1}(t) \\ \mathbf{u}^{m_2}(t) \\ \vdots \\ \mathbf{u}^{m_d}(t) \end{pmatrix}, \quad (1)$$

where $\mathbf{B} \in \mathbb{R}^{K \times K}$ denotes the autoregressive coefficient matrix at lag 1 for which the total number of time series K is given by $K = k_L + m_1 \cdot k_1 + m_2 \cdot k_2 + \dots + m_d \cdot k_d$. Further, $\{\mathbf{u}_t \in \mathbb{R}^K\}_{t=1}^T$ is a mean zero error vector with nonsingular contemporaneous covariance matrix Σ_u . We assume, without loss of generalization, that all series are mean-centered such that no intercept is included. As for the standard VAR, the ij^{th} entry of \mathbf{B} , denoted by β_{ij} , explains the lagged effect of the j th series on the i th series. The entries of the autoregressive coefficient matrix thus permits one to study one-step-ahead predictive Granger causality, an often investigated feature also in the context of MF-VARs (e.g., Ghysels et al., 2016; Götz et al., 2016). Besides, given the mixed-frequency nature of the variables, it may be of interest to analyze whether knowing the values of the high-frequency variable at time t helps to predict the low-frequency variable during the same time period and vice versa. This form of hidden, contemporaneous Granger causality between high- and low-frequency variables can be derived from the error covariance matrix Σ_u and will be further discussed in Section 2.2.

²Note that we collect all high-frequency observations of one variable and then stack the variables. Ghysels (2016), in contrast, collects all observations during the same high-frequency period and stacks those. We deviate from this notation as our regularized estimator makes use of penalties which are built upon sub-matrices of the autoregressive parameter matrix (see Section 2.1) that can be more compactly represented using our notation.

For notational simplicity, we focus throughout the paper on first-order mixed-frequency VARs, since the information density and the number of estimated coefficients, as demonstrated in Equation (1), are already quite high. Even a MF-VAR_K(1) model requires one to estimate K^2 parameters which quickly becomes large since for a fixed T the parameter vector grows (quadratically) with the number of time series included but also due to the high-per-low frequency observations m_1, \dots, m_d . Extensions to higher-order systems can be easily made. In the remainder, we use matrix notation to compactly express the mixed-frequency VAR. To this end, define

$$\begin{aligned}\bar{\mathbf{y}}_t &= [\mathbf{y}(t)', \mathbf{x}^{m_1}(t)', \dots, \mathbf{x}^{m_d}(t)']' \quad (K \times 1) & \mathbf{Y} &= [\bar{\mathbf{y}}_1, \dots, \bar{\mathbf{y}}_N]' \quad (N \times K) \\ \mathbf{Z} &= [\bar{\mathbf{y}}_0, \dots, \bar{\mathbf{y}}_{N-1}]' \quad (N \times K) & \mathbf{X} &= \mathbf{I}_K \otimes \mathbf{Z} \quad (NK \times K^2) \\ \mathbf{u}_t &= [\mathbf{u}(t)', \mathbf{u}^{m_1}(t)', \dots, \mathbf{u}^{m_d}(t)']' \quad (K \times 1) & \mathbf{U} &= [\mathbf{u}_1, \dots, \mathbf{u}_N]' \quad (N \times K),\end{aligned}$$

where $N = T - 1$ are the number of time points actually available given the mixed-frequency VAR of order $\ell = 1$, \mathbf{I}_K denotes the identity matrix of dimension K and \otimes denotes the Kronecker product. Then the MF-VAR_K(1) can simply be written as $\mathbf{y} = \mathbf{X}\boldsymbol{\beta} + \mathbf{u}$, where $\mathbf{y} = \text{vec}(\mathbf{Y})$, $\boldsymbol{\beta} = \text{vec}(\mathbf{B}')$ and $\mathbf{u} = \text{vec}(\mathbf{U})$ and $\text{vec}(\cdot)$ corresponds to the operator staking the columns of a matrix.

In the classical low-dimensional setting $K < N$, the MF-VAR_K(1) model can be estimated by least squares. However, as the number of parameters grows relative to the time series length T , the least squares estimator becomes unreliable as it results in high variance, overfitting and poor out-of-sample forecast performance. We therefore resort to penalized estimation methods. Many authors have used the lasso penalty (Tibshirani, 1996), which attains so called “patternless” sparsity in the parameter matrices of the VAR (e.g., Hsu et al., 2008; Derimer et al., 2018). We, instead, use the dynamic structure of the MF-VAR model as a valuable source of additional information about the nature of the sparsity pattern. Therefore, we propose a regularized estimation of MF-VARs that translates information about the hierarchical structure of low- and high-frequency variables into a convex regularization procedure that delivers structured sparsity patterns appropriate to the context of mixed-frequency models.

2.1 Hierarchical Structures

In this section, we describe the hierarchical sparsity patterns that arise in the autoregressive coefficient matrix \mathbf{B} of a MF-VAR. We demonstrate the intuition – for ease of notation – with $k_L = k_1 = \dots = k_d = 1$, however, our procedure naturally allows one to apply these hierarchical structure to multiple series. The parameters of the matrix \mathbf{B} can be divided in $(d + 1)^2$ different groups as depicted by the sub-matrices in the left panel of Figure 1. We distinguish three types of sub-matrices capturing respectively *Own-on-Own* (blue), *Higher-on-Lower* (green) and *Lower-on-Higher* (red) effects. The *Own-on-Own* sub-matrices are $m \times m$

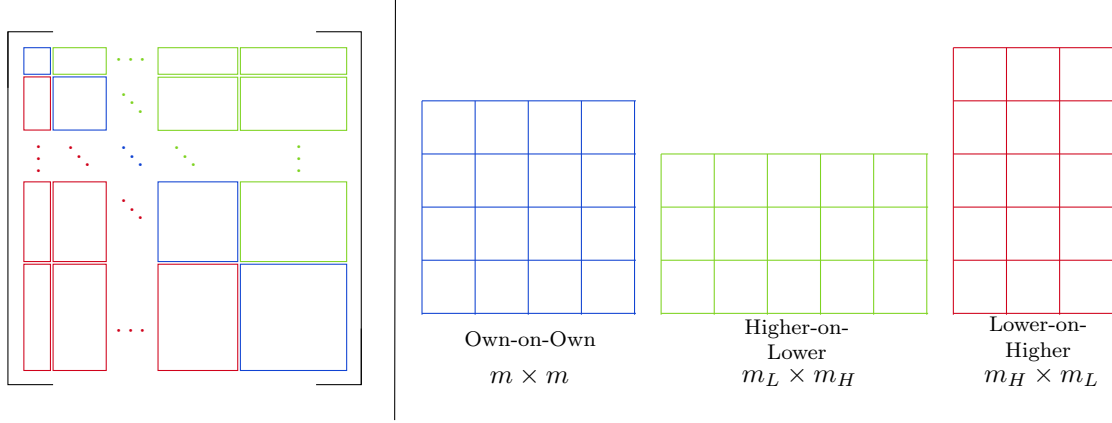


Figure 1: Division of autoregressive coefficient matrix \mathbf{B} into sub-matrices capturing Own-on-Own (blue), Higher-on-Lower (green) and Lower-on-Higher (red) effects.

square matrices that lie on the main diagonal and describe the effects of a series' own lags on itself.³ The *Higher-on-Lower* sub-matrices are short, wide $m_L \times m_H$ matrices, where L and H refer to the corresponding lower- and higher-frequency variable. They lie above the main diagonal and contain the lagged effect of a higher-frequency series onto a series with respective lower frequency. Note that L and H just identify which of the two variable is of higher frequency relative to the other one. Thus, this group does not only contain the effects of the higher-frequency variables onto the variable with the lowest frequency but also describes the interactions between the higher-frequency variables. For instance, in a quarter/month/week-example, these incorporate the effects of the monthly and weekly variable onto the quarterly variable but also the effects of the weekly onto the monthly variable. The *Lower-on-Higher* sub-matrices are long, thin $m_H \times m_L$ matrices. They lie below the main diagonal and contain the lagged effect depicting the effect of a lower-frequency series onto a higher-frequency series.

For each sub-matrix, we impose a hierarchical priority structure for parameter inclusion. Parameters with higher priority within one group should be included in the model before parameters with lower priority within the same group, where the priority value of each parameter depends on how informative the associated regressor is. A priority value of one indicates highest priority for parameter inclusion. More precisely, we introduce a priority value $p_g^{ij} \in \{1, \dots, P_g\}$ for each element ij belonging to parameter group $g = 1, \dots, G$ in the matrix \mathbf{B} to denote its priority of being included in the model. Here, we order the groups in Figure 1 from left to right and top to bottom. For instance, the top left, blue square is group $g = 1$, the green rectangle to the right is group $g = 2$. If $p_g^{ij} < p_g^{i'j'}$ for $i \neq i'$ and $j \neq j'$, we prioritize parameter β_{ij} over $\beta_{i'j'}$ in the model. Note that the hierarchical structure is imposed for each group g individually and hence in each group the priority values start with value 1 (parameters having highest priority) and go up to P_g (parameters having lowest priority). We do not encode structures where certain parameters of one

³We implicitly take $m_L = 1$ for the low-frequency variable.

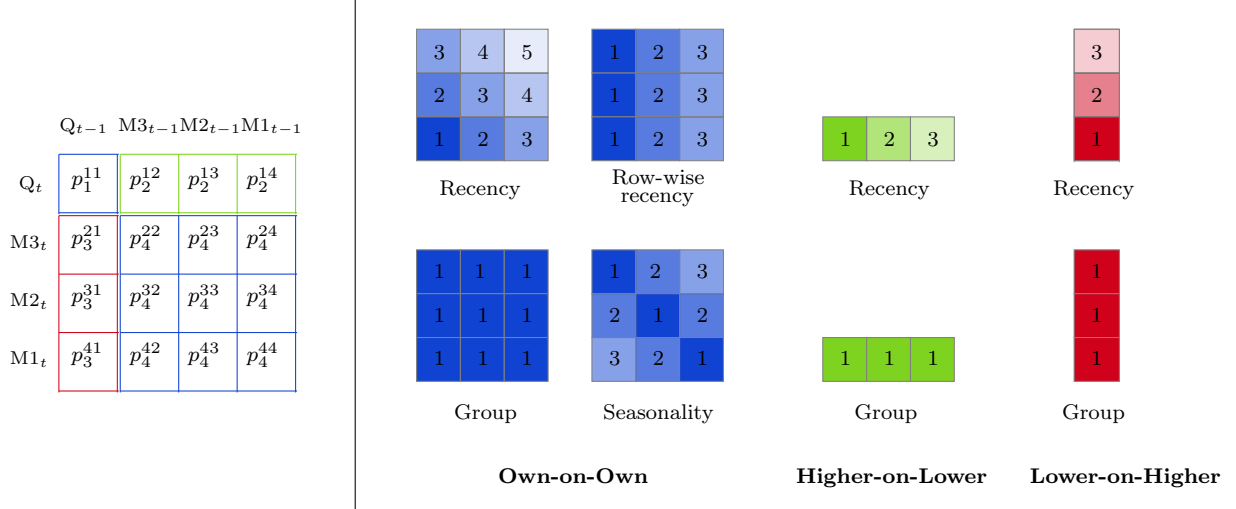


Figure 2: Left panel: Priority values p_g^{ij} , corresponding to each element ij in the autoregressive coefficient matrix \mathbf{B} for a MF-VAR₄(1). Right panel: Different types of penalty structures for parameter groups Own-on-Own, Higher-on-Lower and Lower-on-Higher in a MF-VAR₄(1).

group should enter the model before certain parameters of another group as our aim is to encode priority of parameter inclusion with respect to the effects of one frequency component (Own/Higher/Lower) on another (Own/Higher/Lower).

These hierarchical priority structures are highly general and accommodate various forms of structured sparsity patterns in the autoregressive parameter matrix that researchers or practitioners might want to encourage. While our accompanying convex regularizer works equally well with any hierarchical priority structure, we give special attention to four types of structures. We first discuss two types that are appropriate for all parameter groups and then consider two which are useful for the Own-on-Own group. Note that each parameter group can have its own type of priority structure, so it is possible to combine several ones. For illustration reasons, we will focus on an example with only one quarterly and one monthly variable having a 4×4 coefficient matrix \mathbf{B} and $G = 4$ groups. Figure 2 visualizes the different forms of penalty structures per parameter block for this example.

Recency-based. We set the priority value p_g^{ij} according to the recency of the information the j th time series of $\bar{\mathbf{y}}_{t-1}$ contains relative to the i th series of $\bar{\mathbf{y}}_t$. The more recent the information contained in the lagged predictor, the more informative, and thus the higher its priority of being included in the model. As an example, consider the Higher-on-Lower parameter block (green), where month three of the previous quarter contains the most recent information, followed by month two and then month one. The priority values are thus increasing from left to right. Applying the recency-based priority (specifically for the Higher-on-Lower group) is conceptually similar to using an exponential Almon lag polynomial with decaying shape in a MIDAS regression. Both approaches assume a decaying memory pattern in the economic processes, however, in our

setting, we do not restrict the parameters to a specific nonlinear function.

Group-Lasso. If one would like to encourage sparsity on the entire parameter group, where either all parameters of a group are included in the model or none, one can set the priority value of each coefficient to one. This concept is equivalent to the group lasso (Yuan and Lin, 2006) which has also been used for standard VAR models, see for instance Basu et al. (2015) and Gelper et al. (2016).

Row-wise Recency-based. For Own-on-Own parameter groups (blue), we also consider a row-wise decoupled version of the recency-based priority structure. Instead of looking at the recency of the information with respect to the entire Own-on-Own parameter group, this structure considers the group’s recency structure row-by-row. From the perspective of each month in the current quarter, month three of the previous quarter always contains the most recent information, followed by month two and then month one. Thus, each row has the same priority values which are increasing from left to right.

Seasonality-based. This priority structure can account for the presence of seasonality and is thereby mostly applicable for the higher-frequency components. If stochastic seasonality is present, it imposes the assumption that a high-frequency series own lag, meaning the lag observed at $(t - 1, j)$, is more informative than the other lags observed at $(t - 1, i)$, where $i \neq j$. Moreover, the greater the temporal distance between the other lag from the own lag, the lower its seasonal influence on the dependent variable, thus the lower the priority of being included in the model. Therefore, diagonal elements of the Own-on-Own matrices are prioritized before off-diagonal elements, thereby imposing a “banded” priority structure as the seasonal influence is decreasing.

Remark 2.1. If one were to extend to a MF-VAR $_K(1)$ with multiple time series per frequency component, the total number of groups G becomes $(k_L + k_1 + \dots + k_d)^2$. Then the priority values describing the dependence of the dependent variable having frequency m_i on the independent variable having frequency m_j would be replicated $k_i \times k_j$ times. E.g., in a setting with two quarterly and three monthly variables, the priority values describing the effect of monthly series on quarterly series are replicated six times.

2.2 Nowcasting Restrictions

The hidden contemporaneous links between high- and low-frequency variables can be investigated in the covariance matrix Σ_u of the error terms \mathbf{u}_t in the MF-VAR model (1). Götz and Hecq (2014) test for block diagonality of Σ_u to investigate the null of no contemporaneous Granger causality or, to put it differently, the absence of nowcasting relationships between high- and low-frequency indicators. In the remainder, we refer to contemporaneous Granger causality as “nowcasting causality”. The authors show that the conditional

single equation model (e.g., MIDAS) with contemporaneous regressors can be misleading as it can change the dynamics observed in a MF-VAR system (e.g., Granger causality relations). We do not face this problem since we work with the reduced form MF-VAR and not with a single equation conditional model derived from the MF-VAR.

In the context of our paper, a detailed inspection of the residual covariance matrix $\hat{\Sigma}_u := \frac{1}{T-\ell} \sum_{t=\ell+1}^T \hat{\mathbf{u}}_t \hat{\mathbf{u}}_t'$ of the high-dimensional MF-VAR is interesting for (at least) two reasons. First, from an economic perspective, we aim to investigate whether there exist high-frequency months, weeks or days of some series that nowcast low-frequency variables. Since this is a correlation measure observed in the symmetric blocks of the residual covariance matrix, we obviously cannot point towards a direction of this contemporaneous link. Lütkepohl (2005, pages 45-48) stresses that the “*direction of (nowcasting) causation must be obtained from further knowledge (e.g., economic theory) on the relationship between the variables*”. We can only agree on that. Second, from a statistical perspective, we aim to compare the performance of the MF-VAR from Section 2.1 when additional restrictions on the error covariance matrix are considered. Intuitively, this is a Generalized Least Squares (GLS) type improvement over the “unrestricted” hierarchical MF-VAR.

In our economic application (to be discussed in Section 5), we consider the quarterly real GDP growth as one of the main low-frequency indicators, and are interested in investigating whether some high-frequency monthly (e.g., retail sales) and/or weekly (e.g., money stock, federal fund rate) series can deliver a coincident indicator of GDP growth with the advantage being that they are released earlier. We do not claim that they directly impact GDP but simply that the business cycle movements detected in those high-frequency variables track the fluctuations of the GDP growth well.

To investigate such nowcasting relations, let us assume a single low-frequency variable and decompose Σ_u into four blocks

$$\Sigma_u = \begin{bmatrix} \sigma_{1,1}^2 & \boldsymbol{\sigma}_{\cdot K-1}^{2'} \\ \boldsymbol{\sigma}_{\cdot K-1}^2 & \Sigma_{2:K} \end{bmatrix},$$

with $\Sigma_{2:K}$ the $(K-1) \times (K-1)$ block of Σ_u corresponding to the covariances between errors of the high-frequency variables. It contains both (co)-variances per high-frequency variable (i.e. its main-diagonal blocks) as well as covariances between different high-frequency variables (i.e. its off-diagonal blocks). $\sigma_{1,1}^2$ is the variance of the error of the low-frequency variables. It is a scalar when there is only one variable but in general it is a square matrix. $\boldsymbol{\sigma}_{\cdot K-1}^2$ is a vector, when there is a single low-frequency variable, with the cross-covariances of the errors between low- and high-frequencies. This will be the block we focus on in this paper to detect nowcasting relations between each low-frequency variable and each high-frequency variable.

To detect nowcasting relations, we investigate the existence of a sparse matrix

$$\Sigma_u^* = \begin{bmatrix} \sigma_{1.1}^{*2} & \sigma_{.K-1}^{*2'} \\ \sigma_{.K-1}^{*2} & \Sigma_{2:K}^* \end{bmatrix},$$

where we leave $\sigma_{1.1}^{*2}$ as well as the main-diagonal blocks in $\Sigma_{2:K}^*$ unrestricted.

The sparsity of the block $\sigma_{.K-1}^{*2}$ is our main focus as it allows us to detect nowcasting relations between the low-frequency variables and each of the high-frequency ones. The sparsity in the off-diagonal blocks of $\Sigma_{2:K}^*$ we allow for is not of main economic interest to our nowcasting application with GDP growth as the low-frequency variable, but it may be of interest in other applications and it does facilitate retrieval of a positive definite Σ_u^* matrix (see Section 3.2).

Remark 2.2. The case $\sigma_{.K-1}^{*2} = \mathbf{0}_{(K-1) \times 1}$ (with one low-frequency variable) corresponds to the block diagonality of Σ_u^* and hence the null of no nowcasting causality.

Remark 2.3. Unlike for the autoregressive parameter matrix, we do not impose a hierarchical sparsity structure on $\sigma_{.K-1}^{*2}$ because the middle month could be a better coincident indicator for a quarterly variable than the last month, for instance. Since this is an empirical issue, we prefer to stick to a regularized estimator of the residual covariance matrix that encourages “patternless” sparsity in $\hat{\sigma}_{.K-1}^{*2}$.

Finally, to build our coincident indicator (as used in the empirical Section 5.2), we use a simple procedure which consists of first selecting the variable-period combinations corresponding to non-zero entries in $\sigma_{.K-1}^{*2}$ and subsequently constructing the first principal component.

3 Regularized Estimation Procedure of MF-VARs

3.1 Hierarchical Group Lasso for Structured MF-VAR

To attain the hierarchical structure presented in Section 2.1, we rely on convex penalties. We use the hierarchical group lasso (Zhao et al., 2009; Yan et al., 2017; Nicholson et al., 2020), which is the group lasso (Yuan and Lin, 2006) with a nested group structure. The group lasso uses the sum of (unsquared) Euclidean norms as penalty term to encourage sparsity on the group-level. Then, either all parameters of a group are set to zero or none. By using nested groups, hierarchical sparsity constraints are imposed where one set of parameters being zero implies that another set is also set to zero. We encourage hierarchical sparsity within each group of parameters by prioritizing parameters with a lower priority value over parameters with a higher priority value. The proposed hierarchical group estimator for the MF-VAR model is given by

$$\hat{\beta} = \underset{\beta}{\operatorname{argmin}} \left\{ \frac{1}{2} \|\mathbf{y} - \mathbf{X}\beta\|_2^2 + \lambda_{\beta} \mathcal{P}_{\text{Hier}}(\beta) \right\}, \quad (2)$$

where $\mathcal{P}_{\text{Hier}}(\beta)$ denotes the hierarchical group penalty and $\lambda_\beta \geq 0$ is a tuning parameter.

Before introducing the hierarchical group penalty, recall that we distinguish $g = 1, \dots, G$ parameter groups in the autoregressive parameter matrix and that P_g is the maximum priority value of parameter group g . To impose the hierarchical structure within each parameter group g , we consider P_g nested sub-groups $s_g^{(1)}, \dots, s_g^{(P_g)}$. Group $s_g^{(1)}$ contains all parameters of group g , $s_g^{(2)}$ omits those parameters having priority value one, and finally the last sub-group $s_g^{(P_g)}$ only contains those parameters having the highest priority value P_g . Clearly, a nested structure arises with $s_g^{(1)} \supset \dots \supset s_g^{(P_g)}$. Now, denote $\beta_g^{(p:P_g)} = [\beta_g^{p'}, \dots, \beta_g^{P_g'}]'$, for $1 \leq p \leq P_g$, where β_g^p collects the parameters of group g having priority value p . We are now ready to define the hierarchical penalty function as

$$\mathcal{P}_{\text{Hier}}(\beta) = \sum_{g=1}^G \sum_{p=1}^{P_g} w_{s_g^{(p)}} \|\beta_g^{(p:P_g)}\|_2. \quad (3)$$

The hierarchical structure within each group g is built in through the condition that if $\beta_g^{(p:P_g)} = \mathbf{0}$, then $\beta_g^{(p':P_g)} = \mathbf{0}$ where $p < p'$. Finally, note that we use weights $w_{s_g^{(p)}}$ to balance unequally sized nested sub-groups. We take $w_{s_g^{(p)}} = \text{card}(g) - \text{card}(s_g^{(p)}) + 1$, where $\text{card}(\cdot)$ corresponds to the cardinality. As the cardinality of the sub-groups $s_g^{(p)}$ is decreasing with p , the weights of the nested sub-groups are increasing with p . This implies that sub-groups containing parameters with lower priority, i.e. with older information about the state of the economy, are penalized more and hence are more likely to be set equal to zero.

We propose a proximal gradient algorithm (see e.g., Tseng, 2008) to efficiently solve the optimization problem in Equation (2). The details can be found in Algorithm 1 in Appendix A. A key ingredient of the algorithm concerns the proximal operator $\text{Prox}_{v\lambda\mathcal{P}(\cdot)}$ which has a closed-form solution making it extremely efficient to compute. Indeed, the updates of each hierarchical group $p = 1, \dots, P_g$ correspond to a groupwise soft thresholding operation given by $\max(1 - v\lambda \cdot w_{s_g^{(p)}} / \|\tilde{\beta}_{s_g^{(p)}}\|_2, 0) \tilde{\beta}_{s_g^{(p)}}$ with v being the step size which we set equal to the largest singular value of \mathbf{X} .

Note that Algorithm 1 requires a starting value $\beta[0]$ which we initially set equal to $\mathbf{0}$. While Algorithm 1 is given for a fixed value of the tuning parameter λ , it is standard in the regularization literature to implement it for a decrementing log-spaced grid of λ values. The starting value λ_{\max} is an estimate of the smallest value that sets all coefficients equal to zero. For each smaller λ along the grid, we use the outcome of the previous run as a warm-start for $\beta[0]$.⁴

3.2 Regularized Estimation of Nowcasting Causality Relations

Our main focus is to detect nowcasting relations between the low- and high-frequency variables. We therefore use the lasso-penalty (Tibshirani, 1996) to impose “patternless” sparsity on the covariances between low-

⁴Computer code is available on the GitHub page of the corresponding author (<https://github.com/MarieTernes>).

and high-frequency errors and the covariances between different high-frequency errors (see Section 2.2). The proposed sparse estimator of the covariance matrix is then given by

$$\hat{\Sigma}_u^* = \underset{\Sigma \succ 0}{\operatorname{argmin}} \left\{ \frac{1}{2} \left\| \hat{\Sigma}_u - \Sigma \right\|_F^2 + \lambda_\Sigma \left\| \Sigma^- \right\|_1 \right\}, \quad (4)$$

where $\lambda_\Sigma \geq 0$ is a tuning parameter, Σ^- are the elements of the off-diagonal blocks of Σ . Furthermore, for a matrix \mathbf{A} , $\|\mathbf{A}\|_F = \|\operatorname{vec}(\mathbf{A})\|_F = (\sum_{ij} \mathbf{A}_{ij}^2)^{1/2}$ denotes the Frobenius norm and $\|\mathbf{A}\|_1 = \|\operatorname{vec}(\mathbf{A})\|_1 = \sum_{ij} |\mathbf{A}_{ij}|$ the l_1 -norm.

Remark 3.1. The mere addition of the l_1 -penalty in optimization problem (4) does not guarantee the estimator $\hat{\Sigma}_u^*$ to be positive definite (see Rothman et al., 2009). To ensure its positive definiteness, the constraint $\Sigma \succ 0$ implies that we only consider solutions with strictly positive eigenvalues. Rothman et al. (2009) show that (4) without the constraint $\Sigma \succ 0$ essentially boils down to element-wise soft-thresholding of Σ^- . To be precise, the sparse estimate $\hat{\Sigma}_u^*$ is given by the soft-thresholding rule $\operatorname{sign}(\Sigma^-) \max(|\Sigma^-| - \lambda_\Sigma, 0)$. If the minimum eigenvalue of the unconstrained solution is greater than 0, then the soft-thresholded matrix is the correct solution to (4). However, if the minimum eigenvalue of the soft-thresholded matrix is below 0, we follow Bien and Tibshirani (2011) and perform the optimization using the alternating direction method of multipliers (Boyd et al., 2011), which is implemented in the R function `ProxADMM` of the package `spcov` (Bien and Tibshirani, 2012). Note that similarly to the estimation of the MF-VAR, we solve (4) for a decrementing log-spaced grid of λ_Σ -values.

If one wishes to incorporate the estimated nowcasting relations, the autoregressive parameters can be re-estimated by taking the error covariance matrix into account. This results in a type of generalized least squares estimator of β as given by

$$\hat{\beta}^* = \underset{\beta^*}{\operatorname{argmin}} \left\{ \frac{1}{2} \left\| \mathbf{y}^* - \mathbf{X}^* \beta^* \right\|_2^2 + \lambda_{\beta^*} \mathcal{P}_{\text{Hier}}(\beta^*) \right\}, \quad (5)$$

where $\mathbf{y}^* = \tilde{\Sigma}^{-1/2} \mathbf{y}$, $\mathbf{X}^* = \tilde{\Sigma}^{-1/2} \mathbf{X}$ and $\tilde{\Sigma} = \hat{\Sigma}_u^* \otimes \mathbf{I}_N$.

4 Simulation Study

We assess the performance of the proposed hierarchical group estimator through a simulation study where we compare its performance to three alternatives, namely the ordinary least squares (OLS), the ridge and the lasso. We focus on the hierarchical estimator with the recency-based priority structure for all three types of parameter groups.

The set-up of our simulation study is driven by our empirical application (see Section 5). We generate the data from the MF-VAR with $K = 22$ (one quarterly variable and seven monthly variables) and $T =$

125. We take as parameter matrix the estimated coefficients obtained in the application Section 5.2 which result in a stable MF-VAR. To make a clear distinction between zero and nonzero coefficients, we have set all coefficients smaller than 0.01 to zero. As result, the coefficient matrix does not strictly follow the recency-based hierarchical structure anymore, thereby favoring the hierarchical estimator less compared to its benchmarks. Note that – throughout the paper – we standardized each time series to have sample mean zero and variance one as commonly done in the regularization literature. To reduce the influence of initial conditions on the data generation process (DGP), we burn in the first 300 observations for each simulation run.

We consider three different simulation designs. The first design compares the estimators in terms of their estimation accuracy and variable selection performance of the autoregressive parameter vector. In the second design, we analyze how well the proposed regularization method can detect the nowcasting relations between the low- and high-frequency variables in $\hat{\Sigma}_u^*$. Lastly, the third design compares the point forecasts between the hierarchical estimator and the GLS-type hierarchical estimator. We run $R = 500$ simulations in each simulation design.

4.1 Autoregressive Estimation Accuracy and Variable Selection

We take the error covariance matrix to be the identity matrix and compare estimation accuracy of the autoregressive parameter vector by calculating the mean squared error

$$\text{MSE} = \frac{1}{R} \sum_{r=1}^R \frac{1}{K^2} \sum_{k=1}^{K^2} (\beta_k - \hat{\beta}_k^{(r)})^2,$$

where $\hat{\beta}_k^{(r)}$ refers to the k th element of the estimated parameter vector in simulation run r . To investigate variable selection performance, we use the false positive rate (FPR), the false negative rate (FNR) and Matthews correlation coefficient (MCC):

$$\begin{aligned} \text{FPR} &= \frac{1}{R} \sum_{r=1}^R \frac{FP}{\#(k : \beta_k \neq 0)} & \text{FNR} &= \frac{1}{R} \sum_{r=1}^R \frac{FN}{\#(k : \beta_k = 0)} \\ \text{MCC} &= \frac{1}{R} \sum_{r=1}^R \frac{TP \times TN - FP \times FN}{\sqrt{(TP + FP)(TP + FN)(TN + FP)(TN + FN)}}, \end{aligned}$$

where TP (and TN) are the number of regression coefficients that are estimated as nonzero (zero) and are also truly nonzero (zero) in the model and FP (and FN) are the number of regression coefficients that are estimated as zero (nonzero), but are truly nonzero (zero) in the model. Both FPR and FNR should be as small as possible. The MCC balances the two measures and is in essence a correlation coefficient between the true and estimated binary classifications. It returns a value between -1 and $+1$ with $+1$ representing

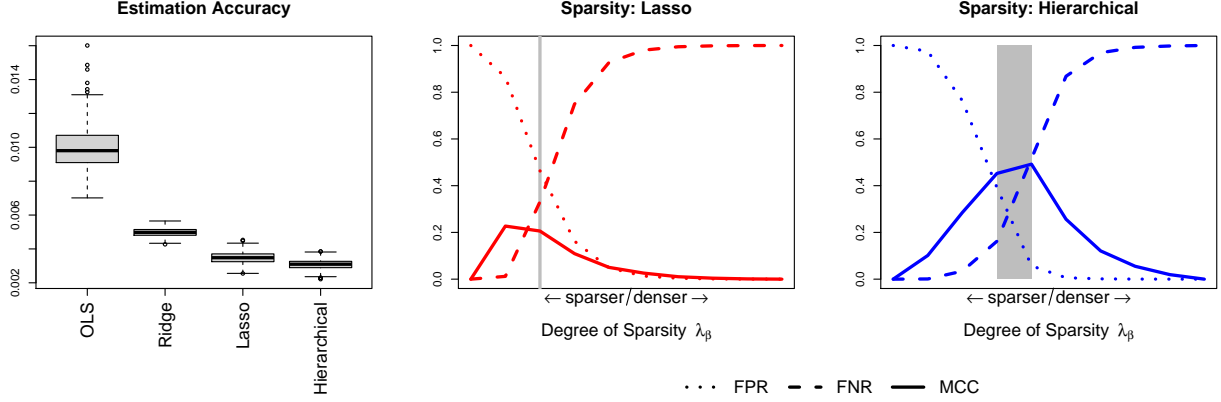


Figure 3: Simulation Study 1: Estimation Accuracy for the four estimators (left) and variable selection performance of lasso and the hierarchical estimator (middle and right)

a perfect prediction, 0 no better than random prediction and -1 complete discrepancy between prediction and observation. For the regularization methods (i.e. the proposed hierarchical estimator, lasso and ridge), we each time use a grid of 10 tuning parameters and select the one that minimizes the MSE between the estimated and true parameter vector.

Results. We first focus on estimation accuracy, see the left panel in Figure 3. The hierarchical estimator generates the lowest estimation errors. It significantly outperforms all others in terms of MSE as confirmed by paired sample t -tests at 5% significance level. OLS suffers as it is an unregularized estimator and thus cannot impose the necessary sparsity on the parameter vector; similarly for ridge which can only perform variable shrinkage but not variable selection. The hierarchical estimator performs slightly better than lasso in terms of MSE, but the difference is less profound since lasso can also handle sparsity.

Secondly, we compare the variable selection performance of lasso and the hierarchical estimator, see the middle and right panel of Figure 3, respectively. The figures plot the average FPR, FNR and MCC for different values of the tuning parameter λ_β . The variable selection performance of the hierarchical estimator is in line with its good performance in terms of estimation accuracy. The maximum MCC lies at roughly 0.5, in comparison to the maximum MCC of lasso which only reaches 0.23. The larger FPR of lasso indicates that its estimate is overly sparse, thereby missing important variables in the model. The larger FNR of the hierarchical estimator in comparison to lasso can be explained by the fact that the DGP does not favour the recency-based structure of the hierarchical estimator. Recall that we have set several small coefficients to zero. Thus, it is possible that within one parameter group we have large coefficients with lower priority and zero coefficients with higher priority. Alternatively, we can have hierarchical groups (all coefficients having the same priority) in which some coefficients are zero and some are large. To estimate and capture those important coefficients, our hierarchical estimator estimates some true zero coefficients as nonzero which

Table 1: Simulation Study 2: Variable selection performance (MCC, FPR, FNR) of nowcasting relations in first row/column of the regularized error covariance matrix. “Estimator” refers to the estimator used to estimate the MF-VAR₂₂(1) and the corresponding residuals from which the covariance matrix is constructed. Standard errors are in parentheses.

Estimator	MCC	FPR	FNR
OLS	0.7111 (0.0052)	0.1937 (0.0058)	0.0960 (0.0064)
Ridge	0.7568 (0.0050)	0.1637 (0.0051)	0.0772 (0.0060)
Lasso	0.7855 (0.0044)	0.1435 (0.0042)	0.0655 (0.0055)
Hierarchical	0.7856 (0.0045)	0.1454 (0.0044)	0.0640 (0.0055)

automatically increases its FNR. Lastly, the grey area in the Figures indicates the 2.5% and 97.5% quantiles of the selected position in the tuning parameter grid across the simulation runs. It illustrates that the maximum MCC lies within the grey area of the hierarchical estimator but does not for lasso.

4.2 Nowcasting Relations

We evaluate the detection of the nowcasting relations. To this end, we set the error covariance matrix to the regularized error covariance matrix estimated in the application Section 5.2. Coefficients smaller than 0.03 are set to zero to again ensure a clear distinction between the zeros and non-zeros. We first estimate the model using the four different estimators, calculate the resulting residual covariance matrix and then compute its regularized version through optimization problem (4). In line with our empirical application, we are mainly concerned with the sparsity pattern of the first row/column, namely the one corresponding to the low-frequency variable. Precisely, we investigate its variable selection performance using MCC, FPR and FNR. We estimate the MF-VAR and covariance matrix of the corresponding residuals for a two-dimensional ($10 \lambda_\beta \times 10 \lambda_\Sigma$) grid of tuning parameters. We select the tuning parameter couple that maximizes the MCC of the regularized covariance matrix in each simulation run.

Results. Table 1 contains the results. The performance across estimators is very similar, but the hierarchical estimator and lasso do perform best. Their MCCs lie at roughly 0.78. Their FPRs are slightly higher than their FNR which implies that the nowcasting relations tend to be estimated too sparsely. On the other hand, the low FNR suggests that in general we do not select variables which do not nowcast the low-frequency variable. Lastly, all estimators perform comparably across the tuning parameter grid for λ_Σ , but the variability around the selected λ_Σ is higher for OLS and ridge than for lasso and the hierarchical estimator.

4.3 Forecast Comparison

We assess whether we can improve upon the best possible forecasting performance of the hierarchical estimator with the help of the GLS-type hierarchical estimator that incorporates the best nowcasting relations.

The error covariance matrix is set to the same matrix as in Section 4.2. We generate time series of length $T = 105$ (as in the empirical forecast application of Section 5.3), fit the models to the first $T - 1$ observations and use the last observation to compute the one-step-ahead mean squared forecast error for series $i = 1, \dots, K$

$$\text{MSFE}_i = \frac{1}{R} \sum_{r=1}^R \left(y_{i,T}^{(r)} - \hat{y}_{i,T}^{(r)} \right)^2,$$

where $y_{i,T}^{(r)}$ is the value of component series i at the time point T in the r^{th} simulation run, and $\hat{y}_{i,T}^{(r)}$ is its predicted value. In line with the empirical application, we focus on forecast accuracy of the first series ($i = 1$) which represents the low-frequency variable of the forecast application. We therefore select the tuning parameter λ_β that minimizes the squared forecast error of the first series. For the selected model, we then estimate its regularized covariance matrix using 10 λ_Σ values and choose the one that maximizes the MCC. Finally, with the selected $\hat{\Sigma}_u^*$, we re-estimate the model according to Equation (5) to compare the forecast performance of the MF-VAR when the additional restrictions on the error covariance matrix are accounted for.

Results. The one-step ahead MSFE for the first series of the hierarchical and GLS-type hierarchical estimator are 0.5508 and 0.5810, respectively. The forecasts performance of the regular hierarchical estimator is significantly better than of the GLS-type estimator as confirmed with a paired sample t-test at 1% significance level. The addition of the nowcasting relation may not improve the forecast because the values of the covariances in the covariance matrix of the DGP, particularly of the first row/column, are relatively small in absolute terms.⁵

Moreover, it is important to point out that the running time for the estimation of the restricted version is substantially larger than for the unrestricted version. Thus, even if the covariance matrix would be denser, there is a clear trade-off between forecast accuracy and computational efficiency one needs to make.

5 Macroeconomic Application

We investigate a high-dimensional MF-VAR for the U.S. economy. We use data from Quarter 3, 1987 until Quarter 4, 2018 ($T = 126$) on various aspects of the economy: amongst others output, income, prices and employment, see Table 2 for an overview. The quarterly and monthly time series are directly taken from the FRED-QD and FRED-MD data-sets which are available at the Federal Reserve Bank of St. Louis FRED database (see McCracken and Ng, 2016, 2020 for more details). The weekly time series are additionally retrieved from the FRED database. The FRED-MD and -QD datasets contain transformation codes to make the data approximately stationary (see column “T-code” in Table 2) which we apply to all series.

⁵The median of the absolute covariances in the first row/column lies at 0.0927 and the maximum absolute covariance is 0.2046.

Table 2: Data description table. Column T-code denotes the data transformation applied to a time-series, which are: (1) not transformed, (2) Δx_t , (3) $\Delta^2 x_t$, (4) $\log(x_t)$, (5) $\Delta \log(x_t)$, (6) $\Delta^2 \log(x_t)$. Columns $K = 22$, $K = 55$ and $K = 91$ indicate whether and at which frequency the variable was included in the model.

FRED Code	Description	T-code	$K = 22$	$K = 55$	$K = 91$
GDPC1	Real Gross Domestic Product	5	Q	Q	Q
RPI	Real Personal Income	5		M	M
CMRMTSPLx	Real Manufacturing and Trade Industries Sales	5		M	M
RETAILx	Retail and Food Services Sales	5		M	M
HOUST	Housing Starts: Total	4	M	M	M
INDPRO	IP Index	5	M	M	M
CUMFNS	Capacity Utilization: Manufacturing	2	M	M	M
UNRATE	Civilian Unemployment Rate	2	M	M	M
PAYEMS	All Employees: Total nonfarm	5	M	M	M
USFIRE	All Employees: Financial Activities	5	M	M	M
CLAIMSx	Initial Claims	5		M	W
CPIAUCSL	CPI : All Items	6	M	M	M
CPIULFSL	CPI : All Items Less Food	6		M	M
PCEPI	Personal Cons. Expend.: Chain Index	6		M	M
WPSFD49207	PPI: Finished Goods	6		M	M
OILPRICEx	Crude Oil	6		M	M
M2SL	M2 Money Stock	6		M	W
FEDFUNDS	Effective Federal Funds Rate	2		M	W
S&P 500	S&P's Stock Price Index	5		M	W

To evaluate the influence of additional variables and the inclusion of higher-frequency components, we estimate three MF-VAR models:⁶ The small MF-VAR ($K = 22$) consists of the quarterly variable at interest – real GDP (*GDPC1*) – and seven monthly variables focusing on (industrial) production, employment and inflation. The medium MF-VAR ($K = 55$) contains the small group and eleven additional monthly variables containing further information on different aspects of the economy including financial variables. The large MF-VAR incorporates the variables of the medium group and replaces four monthly variables (*CLAIMSx*, *M2SL*, *FEDFUNDS*, *S&P 500*) with their equivalent weekly series. See columns “ $K = 22$ ”, “ $K = 55$ ” and “ $K = 91$ ” of Table 2. To ensure that $m_2 = 12$ in the large MF-VAR, we consider all months with more than four weekly observations and disregard the excessive weeks at the beginning of the corresponding month in line with Götz et al. (2016).

We aim to investigate several aspects. First, we focus on the autoregressive parameter estimates of the hierarchical estimator to investigate the predictive Granger causality relations between the series through a network analysis. Second, we concentrate on nowcasting and investigate whether some high-frequency monthly and/or weekly economic series nowcast quarterly U.S. GDP growth and thus can deliver a coincident indicator of GDP growth. Third, we perform an out-of-sample rolling-window forecast exercise. Finally, we investigate whether incorporating more high-frequency components in the model MF-VAR leads to a more

⁶We label the three MF-VAR models as “small”, “medium” and “large” to compare their relative size. Note that even the small MF-VAR is large in traditional time series analysis.

accurate coincident indicator and/or better forecast performance. Note that for ease of the discussion of the results, we follow the variable classification of McCracken and Ng (2016) which can be found in Table 8 in Appendix B.1.

5.1 Autoregressive Effects

We first investigate predictive Granger causality relations. To that end, we estimate the MF-VAR using the hierarchical estimator with recency-based priority structure (seasonally adjusted data are used) for all parameter groups and a grid of 10 tuning parameters λ_β . The tuning parameter is selected using rolling window time series cross-validation with window size T_1 . For each rolling window whose in-sample period ends at time $t = T_1, \dots, T-1$, we first standardize each time series to have sample mean zero and variance one using the most recent T_1 observations, thereby taking possible time variations in the first and second moment of the data into account (see e.g., the Great Moderation Campbell, 2007; Stock and Watson, 2007). Given the evaluation period $[T_1, T]$, we use the one-step-ahead mean-squared forecast error as a cross-validation score:

$$\text{MSFE} = \frac{1}{K(T - T_1)} \sum_{i=1}^K \sum_{t=T_1+1}^T (y_{i,t} - \hat{y}_{i,t})^2,$$

where $\hat{y}_{i,t}$ is the forecast for series i at time $t = T_1 + 1, \dots, T$. We set the effective sample size $T_1 = 105$, leaving us with 20 observations for tuning parameter selection. We first discuss the results for the small MF-VAR, then summarize the findings for the medium and large MF-VARs.

Small MF-VAR. Figure 4(a) depicts the estimated autoregressive coefficient matrix of the hierarchical estimator; 195 of the 484 coefficients (roughly 40%) are estimated as non-zero as indicated by the coloured cells. Figure 4(b) visualizes the same results through a directed network. The vertices represent the variables, the edges the nonzero autoregressive coefficients. The edge’s width is proportional to the absolute value of the estimate. The colors of the vertices and their outgoing edges indicate to which macroeconomic group in McCracken and Ng (2016) the variable and its outgoing effect belong. Furthermore, we summarize the linkages between the macroeconomic categories in Table 3. The columns reflect a macroeconomic category’s out-degree (influence), the rows its in-degree (responsiveness).

We first concentrate on our main variable of interest *GDPC1*. Eight variables contribute towards its prediction (see first row of Figure 4(a) or incoming edges in panel (b)). Most influential is the macroeconomic group Output & Income as month three and two are included for both variables (*INDPRO* and *CUMFNS*). The three variables related to employment (*UNRATE*, *PAYEMS* and *USFIRE*) and *HOUST* are each selected with their third monthly component. Besides, 14 economic variables are influenced by lagged *GDPC1* (see first column of Figure 4(a) or outgoing red edges of its vertex in panel (b)). The Employment category has the most incoming edges, nevertheless, the most prominent (thicker) red edges indicate that

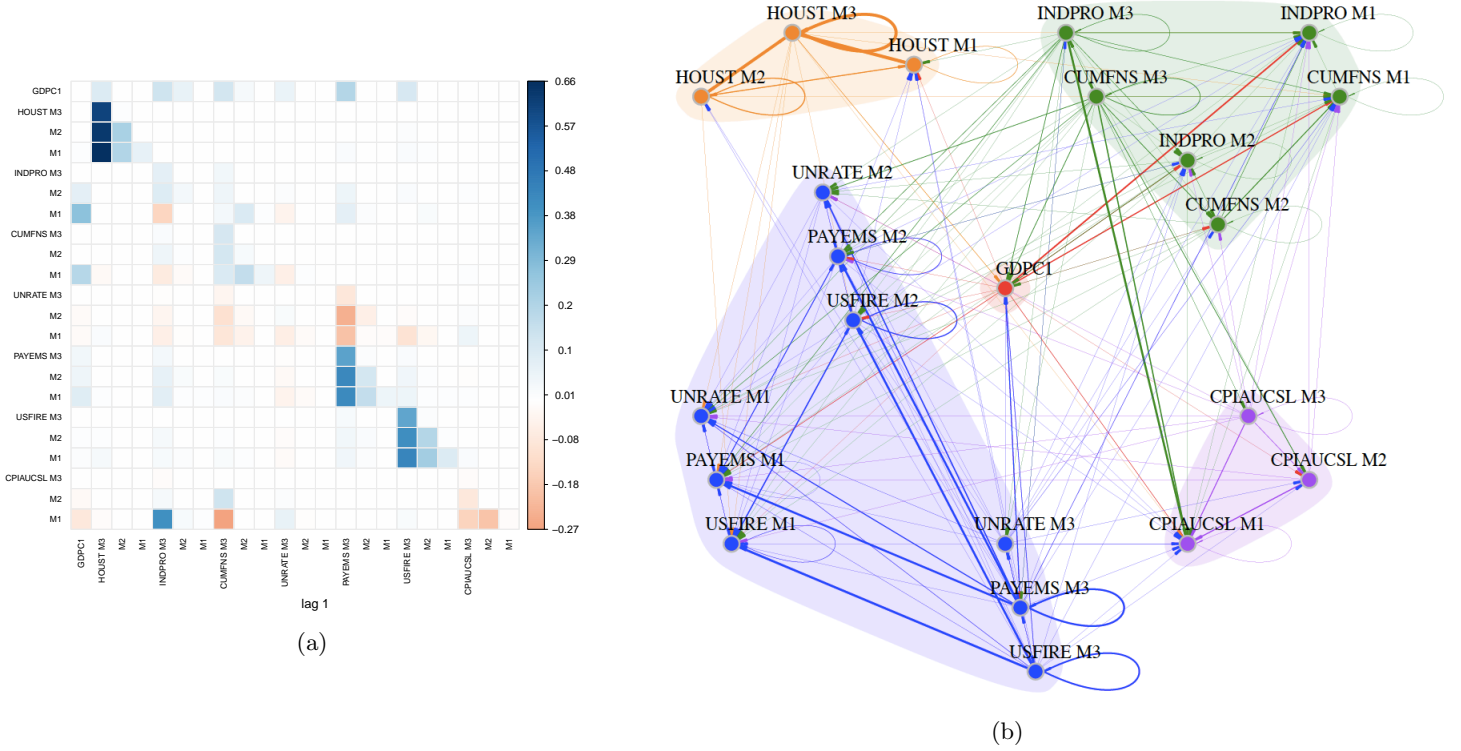


Figure 4: Small ($K = 22$) MF-VAR: Autoregressive coefficients as a matrix (panel (a)) or as a directed network (panel (b)). The vertices represent the variables, the edges the nonzero coefficients. The edges' width are proportional to the absolute value of the estimates. Coloring of the vertices and their outgoing edges indicate the macroeconomic categories

GDPC1 contributes the most to month one of *INDPRO* and *CUMFNS* (i.e. the Output & Income group).

Next, we focus on the linkages between macroeconomic groups containing the higher-frequency variables in Table 3. The categories Output & Income and Employment are strongly connected with each other and have the most outgoing edges, even when taking into account that these groups contain more than one monthly variable. Output & Income also contributes to the prediction of Prices and Employment towards Prices as well as Housing. While Prices play a substantial role for Output & Income and Employment, Housing is more relevant for Employment than it is for Output & Income.

Finally, we inspect the linkages within each macroeconomic group (see Table 3, diagonal entries). Employment and Housing display the highest within-group interaction. Zooming in on *PAYEMS* or *USFIRE* in Figure 4 one can clearly see that their own lagged effects are the strongest, despite them belonging to a group containing more than one high-frequency variable. This indicates that within the macroeconomic groups, a series' own lags remain to be most informative.

When focussing again on the network, we find that the third months of the variables have the most outgoing edges, whereas the first months have the most incoming edges. This is a logical consequence of the "recency-based" priority structure that we imposed.

Table 3: Small ($K = 22$) MF-VAR: Linkages between macroeconomic group. Entry (i, j) indicates the number of edges from group j to group i .

To/From	GDP	Output & Income	Housing	Employment	Prices	<i>In-degree</i>
GDP	0	4	1	3	0	8
Output & Income	4	23	3	14	6	50
Housing	1	1	8	6	0	16
Employment	7	26	5	51	7	96
Prices	2	9	1	8	5	25
<i>Out-degree</i>	14	63	18	82	18	195

Table 4: Medium ($K = 55$) MF-VAR: Linkages between macroeconomic group. Entry (i, j) indicates the number of edges from group j to group i .

To / From	GDP	Output & Income	Sales	Housing	Employment	Prices	Money	Interest Rate	Stock Prices	<i>In-degree</i>
GDP	0	3	2	1	5	1	2	1	1	16
Output & Income	5	36	18	2	29	28	8	9	15	150
Sales	4	18	11	4	31	27	6	6	6	113
Housing	1	1	2	8	6	0	1	0	0	19
Employment	9	37	20	8	73	31	11	14	10	213
Prices	8	46	25	5	43	67	8	15	15	232
Money	1	9	3	1	9	12	4	3	3	45
Interest Rate	1	5	8	2	14	8	2	6	5	51
Stock Prices	1	8	4	1	5	13	1	1	3	37
<i>Out-degree</i>	30	163	93	32	215	187	43	55	58	876

Medium and Large MF-VAR. To evaluate the influence of dimensionality, we now compare our results to the two larger MF-VARs. Their networks are given in Figures 6 and 7 in Appendix B.2, whereas Tables 4 and 5 present the linkages between the macroeconomic categories, respectively. The medium MF-VAR has 876 out of 3025 non-zero coefficients (30%), the large MF-VAR 1220 out of 8281 (only 15%). The increase in dimensionality thus induces a higher degree of selectiveness.

Looking at the influencers of $GDPC1$, we find that the majority of the variables selected for $K = 22$ are also selected for the medium and large MF-VAR. In addition, the monetary ($M2SL$) and financial variables ($FEDFUNDS$ and $S\&P500$) as well as two monthly variables related to sales ($CMRMTSPLx$ and $RETAILx$) deem to be relevant. Apart from month three of $OILSPRICEx$, no variables related to prices are selected for the prediction of GDP growth. This coincides with the results for the small MF-VAR where $CPIAUCSL$ also only had minor influence. Similarly, the variables that $GDPC1$ influences in the medium and large system overlap with the selected ones in the small system. Particularly, $GDPC1$ strongly contributes to the prediction of the variables in the macroeconomic groups Output & Income, illustrated by its thick outgoing red edges, and Employment, indicated by the most incoming red edges.

Next we focus on the linkages between the macroeconomic groups. For the medium MF-VAR, Table 4 underlines that Output & Income, Sales, Employment and Prices are highly interconnected. Moreover, the group Interest Rates influences the groups Employment and Prices. The latter one is not surprising

Table 5: Large ($K = 91$) MF-VAR: Linkages between macroeconomic group. Entry (i, j) indicates the number of edges from group j to group i . Weekly variables are separated.

To / From	GDP	Output & Income	Sales	Housing	Employ- ment	Prices	CLAIMSx	Money	Interest Rate	Stock Prices	<i>In- degree</i>
GDP	0	4	2	1	4	1	1	2	2	2	19
Output & Income	6	37	21	4	23	31	11	15	17	16	181
Sales	4	20	12	4	22	25	8	12	12	12	131
Housing	1	1	2	8	6	0	0	1	1	1	21
Employment	7	30	21	5	52	16	10	13	15	10	179
Prices	8	46	27	5	30	73	24	28	25	29	295
CLAIMSx	2	15	9	3	10	19	9	7	9	5	88
Money	1	17	9	4	14	23	8	10	9	9	104
Interest Rate	1	20	10	3	17	12	7	9	13	10	102
Stock Prices	2	12	12	4	10	27	5	10	9	9	100
<i>Out-degree</i>	32	202	125	41	188	227	83	107	112	103	1220

as *FEDFUNDS* is usually set to control inflation, hence one can expect changes in the previous quarter to aid in predicting inflation, measured by changes in prices. A similar argument supports the interconnection between Prices and Money. When looking at the diagonal entries of Table 4, we notice that similarly to the small MF-VAR, the groups Employment, Housing and Output & Income have a high within-groups interaction. In contrast to the small system, the within-group linkages among Prices highly increases, which is likely due to the addition of four price variables. The introduction of the weekly variables in the large system does not change the relations among the macroeconomic categories (see Table 5).

5.2 Coincident Indicators

We investigate whether some high-frequency monthly and/or weekly economic series nowcast quarterly U.S. GDP growth and thus can deliver a coincident indicator of GDP growth. More specifically, we analyze how the performance of the indicator is influenced through (i) the formalization of “sparse” nowcasting relations in the MF-VAR in comparison to a naive approach of constructing a coincident indicator based on the first principal component of *all* high-frequency variables and (ii) the number of high-frequency components included in the model.

To construct the coincident indicator, we first estimate the MF-VAR using the hierarchical estimator as in Section 5.1. Secondly, we compute the regularized $\hat{\Sigma}_u^*$ from the MF-VAR residuals. We then select the high-frequency variables having a non-zero covariance element in the GDP column and construct the first principal component of the corresponding correlation matrix.⁷ We estimate the MF-VAR and corresponding covariance matrix of the MF-VAR residuals for a two-dimensional (10×10) grid of tuning parameters λ_β and λ_Σ . We report the results for the tuning parameter couple that maximizes the correlation between the most parsimonious coincident indicator and GDP growth.⁸

⁷Alternatively, one could construct a coincident indicator by Partial Least Squares. The results are comparable.

⁸As we cannot select according to MCC, we use the maximum correlation as proxy. Since we standardize GDP growth and the coincident indicator this is equivalent to selecting the tuning parameter that minimizes the MSE between both.

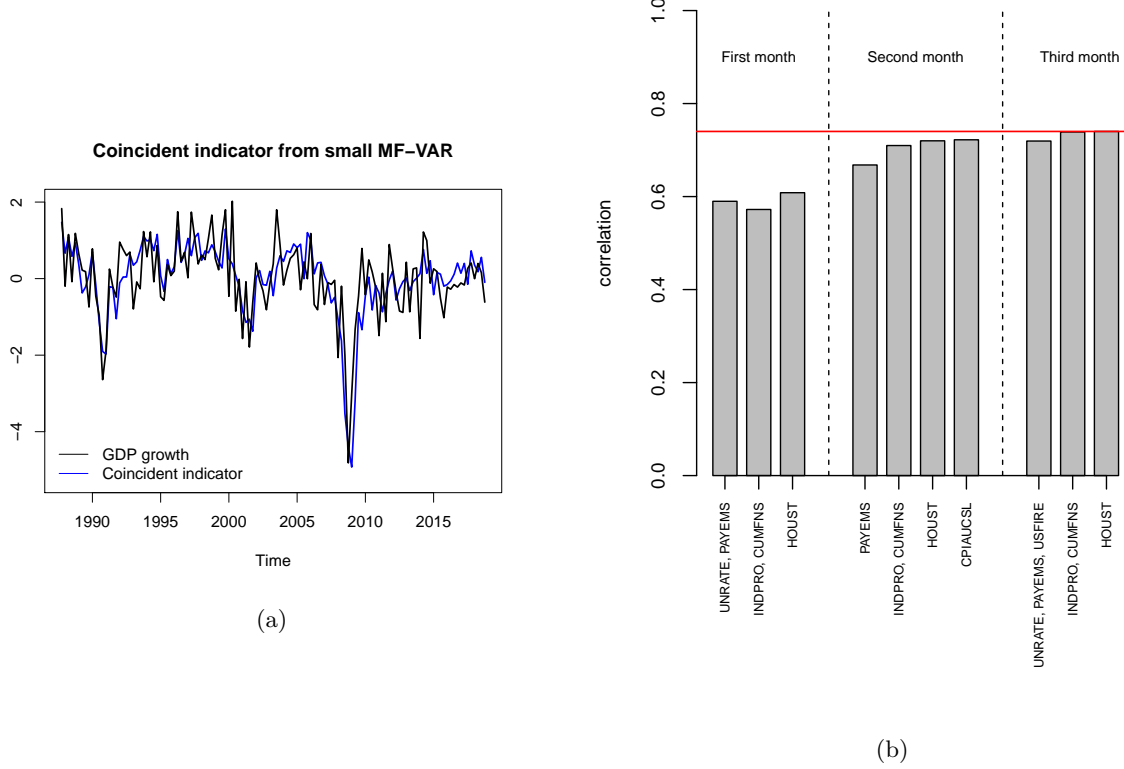


Figure 5: Small ($K = 22$) MF-VAR: Panel (a): U.S. GDP growth versus coincident indicator. Panel (b): Correlation between U.S. GDP growth and different coincident indicators by data release. The red line indicates the correlation between U.S. GDP growth and the coincident indicator constructed from all selected nowcasting relations from the entire quarter.

Small MF-VAR. Figure 5(a) plots the (standardized) U.S. GDP growth (black) against the (standardized) coincident indicator (blue) for the small MF-VAR that maximizes the correlation to a value of 0.7401. The indicator tracks the movements of the GDP growth fairly well. The selected monthly variables from which the first principal component has been constructed are listed on the x-axis of Figure 5(b). Thus, 16 out of the 21 high-frequency variables are selected, since their corresponding covariance with GDP growth is estimated as non-zero. Each variable is included with at least one monthly component. The variables related to Housing (*HOUST*) and Output & Income (*INDPRO* and *CUMFNS*) follow the fluctuations of GDP growth particularly well as all three months are selected. The variables measuring Employment (*UNRATE*, *PAYEMS* and *USFIRE*) have varying levels of contribution. Lastly, the second month of *CPIAUCSL*, which measures price changes, is also chosen.

For comparison, a coincident indicator constructed from *all* high-frequency variables would result in a correlation of 0.7199. Capturing the nowcasting relations in a MF-VAR where the lagged and instantaneous dynamics are separated, thus increases the correlation by 2 percentage points.

Furthermore, the correlations with GDP growth are fairly stable across the two-dimensional grid of tuning

Table 6: Correlation between U.S. GDP growth and the coincident indicators for the small ($K = 22$), medium ($K = 55$) and large ($K = 91$) MF-VAR groups.

Type of coincident indicator	$K = 22$	$K = 55$	$K = 91$
Nowcasting relations M1	0.6083	0.5075	0.5703
Nowcasting relations M1 + M2	0.7221	0.7560	0.7606
All nowcasting relations	0.7401	0.7689	0.7724
All variables	0.7199	0.7542	0.7409

parameters. In roughly half of the cases, the correlation is at least as high as the one computed from all high-frequency variables. Our findings are thus rather robust to a different choice of selection criterion for the tuning parameters. Time series cross-validation (with one-step-ahead MSFE as a cross-validation score), for instance, results in a correlation of 0.7318 between the coincident indicator and GDP growth; detailed results are available from the authors upon request.

GDPC1 is typically released with a relatively long delay (usually one month after the quarter), whereas the monthly variables are released in blocks at different dates throughout the following month.⁹ For instance, the previous month’s *UNRATE*, *PAYEMS* and *USFIRE* are typically released on the first Friday of the following month, whereas the remaining variables are only available around the middle of the month. We follow the release scheme of Giannone et al. (2008) to study the marginal impact of these data releases on the construction of our coincident indicator. Note that we do not take data revisions into account. Hence, our vintages are “pseudo” real-time vintages rather than true real-time vintages.

Figure 5(b) illustrates the achieved correlation between GDP growth and the coincident indicator, updated according to the release dates of the selected variables. As such, the first coincident indicator only uses month one for *UNRATE* and *PAYEMS*, whereas the last one is constructed from all selected variables and its correlation with GDP growth is indicated by the red horizontal line. The figure shows that intra-quarter information matters. The second month releases have a large impact on the accuracy of the coincident indicator. Particularly, the addition of the variables *INDPRO* and *CUMFNS* raises the correlation significantly. In fact, it is possible to construct an almost equally reliable indicator with the data from month one and two compared to one constructed with the data from the entire quarter. Hence, it is possible to build a reliable coincident indicator roughly 1.5 months before the first release of GDP, thereby accounting for the publishing lag of approximately half a month for the monthly series.

Medium and Large MF-VAR. Table 6 summarizes the correlations between GDP growth and the coincident indicators constructed from the different VAR systems. The correlation for the large system (0.7724) is slightly higher than for the medium MF-VAR (0.7689) and both outperform the small system (0.7401).

⁹In our case, the variables belonging to the same macroeconomic category (McCracken and Ng, 2020) are published on the same day of the month.

Table 7: Rolling out-of-sample one-step-ahead MSFE of *GDPC1* for AR, RW and the hierarchical estimator (with small ($K = 22$), medium ($K = 55$) and large ($K = 91$) MF-VAR groups). Forecast methods in the 85% Model Confidence Set (MCS) are in bold. Standard errors are in parentheses.

	Univariate		Multivariate Hierarchical		
	AR	RW	$K = 22$	$K = 55$	$K = 91$
MSFE	0.4006	0.6870	0.1540	0.1277	0.1718
	(0.1891)	(0.3638)	(0.0748)	(0.0598)	(0.1012)

Full details on the medium and large MF-VAR are available in Appendix B.2: Figures 8(a) and 9(a) show that both indicators behave similarly and can better pick up the drop in GDP growth during the financial crisis than the coincident indicator of the small system. Many of the variables selected for the coincident indicator of the small MF-VAR are also selected for the two larger MF-VARs (see Figures 8(b) and 9(b)): There is a clear focus on variables related to (industrial) output, sales and employment whereas variables measuring price changes have a smaller influence. Furthermore, the number of included high-frequency variables of the large system is smaller than for the medium MF-VAR. Hence, it is valuable to incorporate even higher-frequency variables, but the mere addition of variables does not lead to a larger correlation, emphasizing that selection is important.

Indeed, Table 6 illustrates that the advantage of selecting the nowcasting relations in the MF-VARs persists as the correlation achieved from the first principal component with all variables is lower. Lastly, the coincident indicator constructed from the selected variables from month one and two performs comparable to the one constructed from all selected variables, in line with our finding for the small MF-VAR.

5.3 Forecast Comparison

Although the main focus of this paper does not lie on forecasting, we still end with a small out-of-sample rolling-window forecast exercise, similar to the one performed in Section 4.3. We use a rolling-window set-up with window size $T_1 = 105$, providing us 20 quarterly observations for forecast comparison. For each rolling window, we select the value of λ_β that minimizes the one-step-ahead squared forecast error for our main variable of interest *GDPC1*. The MSFE for *GDPC1* for the unrestricted hierarchical estimator across all MF-VARs is given in Table 7.¹⁰ We compare the forecast performance of the hierarchical estimator to the random walk (RW) model and the Autoregressive model with one lag (AR(1)) as two popular and simple univariate benchmarks.

The hierarchical estimator outperforms the AR and RW across the three MF-VARs, as confirmed by the Model Confidence Set procedure (Hansen et al., 2011), thereby indicating that higher-frequency variables are predictive for GDP growth. The medium MF-VAR attains the lowest MSFE, followed by the small

¹⁰We have also performed the forecasting exercise with the restricted hierarchical estimator imposing the nowcasting restrictions (through GLS). In line with your simulation study in Section 4.3, the GLS version did not result in an improved point forecast and thus is omitted.

MF-VAR. We find that moving away from small MF-VAR leads to better forecast accuracy. In contrast, the mere addition of many more variables in the large MF-VAR deteriorates the forecast accuracy.

6 Conclusion

We introduce a convex regularization method tailored towards the hierarchically ordered structure of mixed-frequency VARs. To this end, we use a group lasso with nested groups which permits various forms of hierarchical sparsity patterns that allows one to discriminate between recent and obsolete information. Our simulation study shows that the proposed regularizer can improve estimation and variable selection performance. Furthermore, nowcasting relations can be detected from the sparsity pattern of the covariance matrix of the MF-VAR errors. Those high-frequency variables that nowcast the low-frequency variables, as evident from their non-zero contemporaneous link, can deliver a coincident indicator of the low-frequency variable. Constructing coincident indicators from a group of selected variables rather than all permits policy makers to get an earlier grasp of the state of the economy, as can be seen from our economic application on U.S. GDP growth. Our MF-VAR with weekly data can for instance also be used to nowcast GDP during the Covid pandemic using weekly indicators (see Lewis et al., 2020).

References

- Andreou, E., Gagliardini, P., Ghysels, E., and Rubin, M. (2019). Inference in group factor models with an application to mixed-frequency data. *Econometrica*, 87(4):1267–1305.
- Babii, A., Ghysels, E., and Striaukas, J. (2020). Machine learning time series regressions with an application to nowcasting. *arXiv preprint arXiv:2005.14057*.
- Barigozzi, M. and Brownlees, C. (2019). Nets: Network estimation for time series. *Journal of Applied Econometrics*, 34(3):347–364.
- Basu, S., Shojaie, A., and Michailidis, G. (2015). Network Granger causality with inherent grouping structure. *The Journal of Machine Learning Research*, 16(1):417–453.
- Bien, J. and Tibshirani, R. (2012). **spcov**: *Sparse Estimation of a Covariance Matrix*. R package version 1.01.
- Bien, J. and Tibshirani, R. J. (2011). Sparse estimation of a covariance matrix. *Biometrika*, 98(4):807–820.
- Boyd, S., Parikh, N., Chu, E., Peleato, B., and Eckstein, J. (2011). *Distributed optimization and statistical learning via the alternating direction method of multipliers*, volume 3 of 1. Foundation and Trends in Machine Learning.

- Brave, S. A., Butters, R. A., and Justiniano, A. (2019). Forecasting economic activity with mixed frequency BVARs. *International Journal of Forecasting*, 35(4):1692 – 1707.
- Callot, L. A., Kock, A. B., and Medeiros, M. C. (2017). Modeling and forecasting large realized covariance matrices and portfolio choice. *Journal of Applied Econometrics*, 32(1):140–158.
- Campbell, S. D. (2007). Macroeconomic volatility, predictability, and uncertainty in the great moderation: Evidence from the survey of professional forecasters. *Journal of Business & Economic Statistics*, 25(2):191–200.
- Derimer, M., Diebold, F. X., Liu, L., and Yilmaz, K. (2018). Estimating Global Bank Network Connectedness. *Journal of Applied Econometrics*, 33(1):1–15.
- Eurostat: Statistics Explained (2014). Glossary:nowcasting. <https://ec.europa.eu/eurostat/statistics-explained/index.php/Glossary:Nowcasting>.
- Foroni, C. and Marcellino, M. (2014). A comparison of mixed frequency approaches for nowcasting Euro area macroeconomic aggregates. *International Journal of Forecasting*, 30(3):554–568.
- Gefang, D., Koop, G., and Poon, A. (2020). Computationally efficient inference in large Bayesian mixed frequency VARs. *Economics Letters*, page 109120.
- Gelper, S., Wilms, I., and Croux, C. (2016). Identifying demand effects in a large network of product categories. *Journal of Retailing*, 92(1):25–39.
- Ghysels, E. (2016). Macroeconomics and the reality of mixed frequency data. *Journal of Econometrics*, 193(2):294–314.
- Ghysels, E., Hill, J. B., and Motegi, K. (2016). Testing for Granger causality with mixed frequency data. *Journal of Econometrics*, 192(1):207–230.
- Ghysels, E., Santa-Clara, P., and Valkanov, R. (2004). The MIDAS touch: Mixed data sampling regression models. Cirano working papers, CIRANO.
- Giannone, D., Reichlin, L., and Small, D. (2008). Nowcasting: The real-time informational content of macroeconomic data. *Journal of Monetary Economics*, 55(4):665–676.
- Götz, T. B. and Hecq, A. (2014). Nowcasting causality in mixed frequency vector autoregressive models. *Economics Letters*, 122(1):74–78.
- Götz, T. B., Hecq, A., and Smeekes, S. (2016). Testing for Granger causality in large mixed-frequency VARs. *Journal of Econometrics*, 193(2):418–432.

- Hansen, P. R., Lunde, A., and Nason, J. M. (2011). The model confidence set. *Econometrica*, 79(2):453–497.
- Hastie, T., Tibshirani, R., and Wainwright, M. (2015). *Statistical learning with sparsity: the lasso and generalizations*. CRC press.
- Hecq, A., Margaritella, L., and Smeekes, S. (2019). Granger causality testing in high-dimensional VARs: a post-double-selection procedure. *arXiv preprint arXiv:1902.10991*.
- Hsu, N.-J., Hung, H.-L., and Chang, Y.-M. (2008). Subset selection for vector autoregressive processes using lasso. *Computational Statistics & Data Analysis*, 52(7):3645–3657.
- Koelbl, L. and Deistler, M. (2020). A new approach for estimating var systems in the mixed-frequency case. *Statistical Papers*, 61(3):1203–1212.
- Kuzin, V., Marcellino, M., and Schumacher, C. (2011). MIDAS vs. mixed-frequency VAR: Nowcasting GDP in the Euro area. *International Journal of Forecasting*, 27(2):529–542.
- Lewis, D., Mertens, K., and Stock, J. H. (2020). Us economic activity during the early weeks of the sars-cov-2 outbreak. Technical report, National Bureau of Economic Research.
- Lütkepohl, H. (2005). *New introduction to multiple time series analysis*. Springer Science & Business Media.
- Marcellino, M. and Schumacher, C. (2010). Factor MIDAS for nowcasting and forecasting with ragged-edge data: A model comparison for German GDP. *Oxford Bulletin of Economics and Statistics*, 72(4):518–550.
- McCracken, M. W. and Ng, S. (2016). FRED-MD: a monthly database for macroeconomic research. *Journal of Business & Economic Statistics*, 34(4):574–589.
- McCracken, M. W. and Ng, S. (2020). Fred-qd: a quarterly database for macroeconomic research. Technical report, National Bureau of Economic Research.
- McCracken, M. W., Owyang, M., and Sekhposyan, T. (2015). Real-time forecasting with a large, mixed frequency, Bayesian VAR. *FRB St. Louis Working Paper*, (2015-30).
- Nicholson, W. B., Wilms, I., Bien, J., and Matteson, D. S. (2020). High dimensional forecasting via interpretable vector autoregression. *Journal of Machine Learning Research*, 21:1–52.
- Rothman, A. J., Levina, E., and Zhu, J. (2009). Generalized thresholding of large covariance matrices. *Journal of the American Statistical Association*, 104(485):177–186.
- Schorfheide, F. and Song, D. (2015). Real-time forecasting with a mixed-frequency VAR. *Journal of Business & Economic Statistics*, 33(3):366–380.

- Smeeke, S. and Wijler, E. (2018). Macroeconomic forecasting using penalized regression methods. *International Journal of Forecasting*, 34:408–430.
- Stock, J. and Watson, M. (2007). Why has U.S. inflation become harder to forecast? *Journal of Money, Credit and Banking*, 39(1):3–33.
- Tibshirani, R. (1996). Regression shrinkage and selection via the lasso. *Journal of the Royal Statistical Society: Series B (Methodological)*, 58(1):267–288.
- Tseng, P. (2008). On accelerated proximal gradient methods for convex-concave optimization. *submitted to SIAM Journal on Optimization*, 1.
- Yan, X., Bien, J., et al. (2017). Hierarchical sparse modeling: A choice of two group lasso formulations. *Statistical Science*, 32(4):531–560.
- Yuan, M. and Lin, Y. (2006). Model selection and estimation in regression with grouped variables. *Journal of the Royal Statistical Society: Series B (Statistical Methodology)*, 68(1):49–67.
- Zhao, P., Rocha, G., Yu, B., et al. (2009). The composite absolute penalties family for grouped and hierarchical variable selection. *The Annals of Statistics*, 37(6A):3468–3497.

Appendices

A Algorithm

Algorithm 1 Accelerated proximal gradient method

Require: \mathbf{y} , \mathbf{X} , $\mathcal{P}(\beta)$, λ , ε

initialization:

- $\beta[1] \leftarrow \beta[2] \leftarrow \beta[0]$
- step size v which is set equal to the largest singular value of \mathbf{X}

for $r = 3, 4, \dots$ **do**

for $g = 1, \dots, G$ **do**

$$\ddot{\beta}_g \leftarrow \beta_g[r-1] + \frac{r-2}{r+1} (\beta_g[r-1] - \beta_g[r-2])$$

$$\beta_g[r] \leftarrow \text{Prox}_{v\lambda\mathcal{P}(\cdot)}(\ddot{\beta}_g - v\nabla_{\beta_g}\mathcal{L}(\ddot{\beta}_g))$$

$$\text{where } \nabla_{\beta_g}\mathcal{L}(\ddot{\beta}_g) = -(\mathbf{y} - \mathbf{X}_{\beta_g}\ddot{\beta}_g - \mathbf{X}_{\beta_{f>g}}\beta_{f>g}[r-1] - \mathbf{X}_{\beta_{f<g}}\beta_{f<g}[r])'\mathbf{X}_{\beta_g}$$

end for

if $\|\beta[r] - \beta[r-1]\|_\infty \leq \varepsilon$ **then**

break

end if

end for

return $\beta[r]$

B Macroeconomic Application

B.1 Additional Tables

Table 8: Categories of monthly series in the medium ($K = 55$) MF-VAR group, following the grouping of McCracken and Ng (2016) in their Appendix.

Macroeconomic category	FRED Code
Output & Income	RPI, INDPRO, CUMFNS
Sales	CMRMTSPLx, RETAILx
Housing	HOUST
Employment	UNRATE, PAYEMS, USFIRE, CLAIMSx
Prices	CPIAUCSL, CPIULFSL, PCEPI, WPSFD49207
	OILPRICEx
Money	M2SL
Interest rates	FEDFUNDS
Stock prices	S&P 500

B.2 Additional Figures

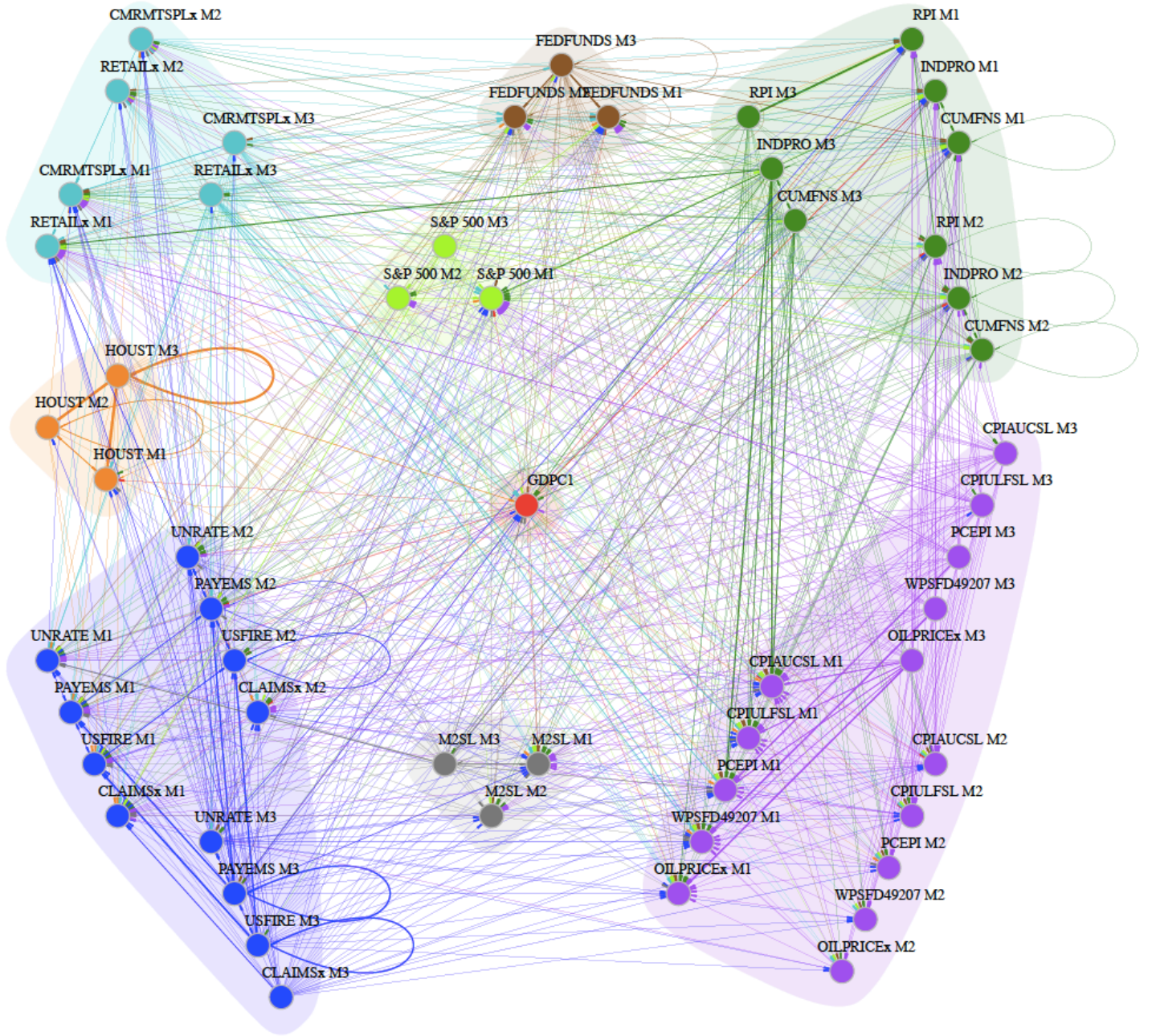


Figure 6: Medium ($K = 55$) MF-VAR: Directed network: the vertices represent the variables, the edges the nonzero coefficients. The edges' width are proportional to the absolute value of the estimates. Coloring of the vertices and their outgoing edges indicate the macroeconomic categories

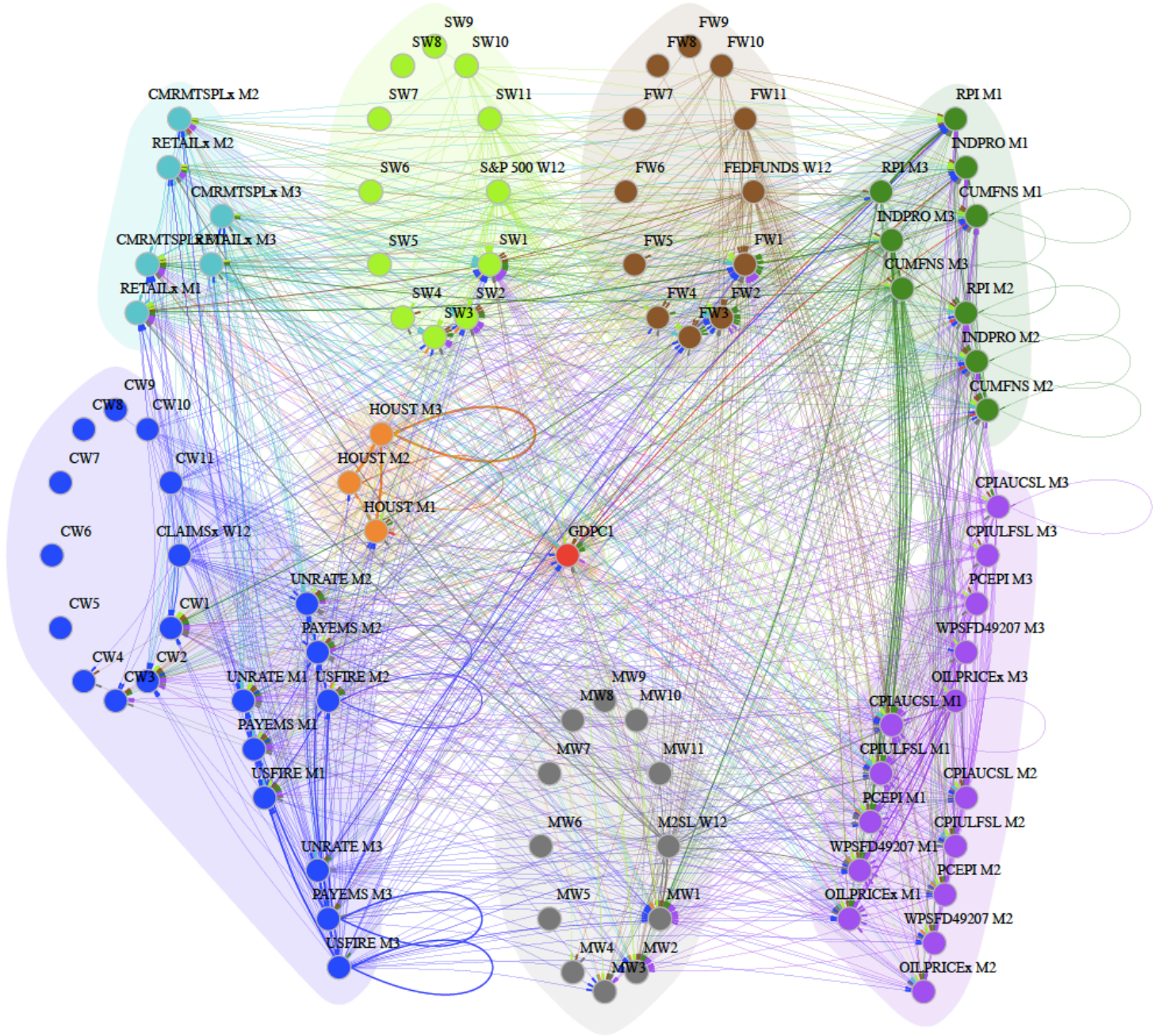
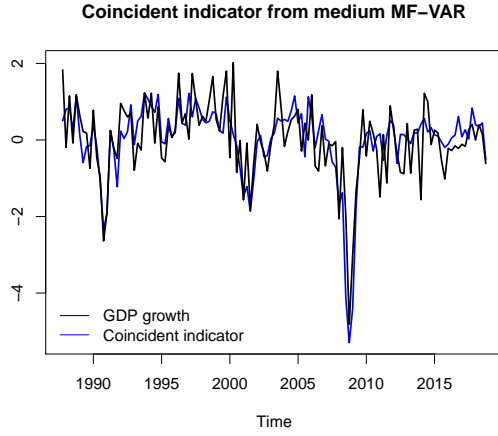


Figure 7: Large ($K = 91$) MF-VAR: Directed network: the vertices represent the variables, the edges the nonzero coefficients. The edges' width are proportional to the absolute value of the estimates. Coloring of the vertices and their outgoing edges indicate the macroeconomic categories

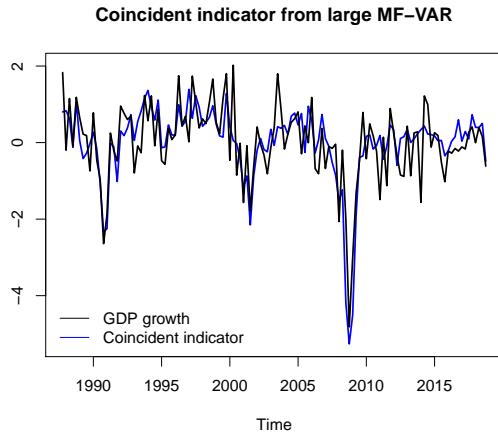


(a)

Variable	Nowcast		
RPI	M1	M2	M3
CMRMTSPLx	M1	M2	M3
RETAILx	M1	M2	M3
HOUST	M1	M2	M3
INDPRO	M1	M2	M3
CUMFNS	M1	M2	M3
UNRATE	M1	M2	M3
PAYEMS		M2	M3
USFIRE		M2	M3
CLAIMSx	M1	M2	M3
CPIAUCSL		M2	
CPIULFSL		M2	M3
PCEPI		M2	
WPSFD49207	M1	M2	
OILPRICEx		M2	
M2SL	M1		M3
FEDFUNDS		M2	M3
S&P 500	M1	M2	M3

(b)

Figure 8: Medium ($K = 55$) MF-VAR: Panel (a): U.S. GDP growth versus coincident indicator. Panel (b): Selected high-frequency variables for the coincident indicator.



(a)

Variable	Nowcast		
RPI		M2	
CMRMTSPLx	M1	M2	M3
RETAILx	M1	M2	M3
HOUST		M2	M3
INDPRO	M1	M2	M3
CUMFNS	M1	M2	M3
UNRATE	M1	M2	M3
PAYEMS		M2	M3
USFIRE		M2	M3
CLAIMSx			
CPIAUCSL		M2	
CPIULFSL		M2	
PCEPI		M2	
WPSFD49207			
OILPRICEx			
M2SL	W12		
FEDFUNDS	W5	W7	W11
S&P 500	W1	W6	

(b)

Figure 9: Large ($K = 91$) MF-VAR: Panel (a): U.S. GDP growth versus coincident indicator. Panel (b): Selected high-frequency variables for the coincident indicator.